

# Investigating the effects of impact directions to improve head injury index

Javad Afshari<sup>1,\*</sup>, Mohammad Haghpanahi<sup>2</sup>, Reza Kalantarinejad<sup>3</sup>, and Abel Rouboa<sup>4</sup>

<sup>1</sup> School of Mechanical Engineering, Iran University of Science and Technology, Tehran 16846-13114, Iran;

Tel: +98 9183171388; [j\\_afshari\\_m@yahoo.com](mailto:j_afshari_m@yahoo.com)

<sup>2</sup> School of Mechanical Engineering, Iran University of Science and Technology, Tehran 16846-13114, Iran;

Tel: +98 21 77240540 [mhaghpanahi@iust.ac.ir](mailto:mhaghpanahi@iust.ac.ir)

<sup>3</sup> Iranian ministry of science and research technology, Aerospace Research Institute, Tehran 14657-74111, Iran;

Tel: +98 2188 366 030; [rezakalantarinezhad@gmail.com](mailto:rezakalantarinezhad@gmail.com)

<sup>4</sup> CIENER-INEGI polo UTAD, University of Trás-os-Montes e Alto Douro, 5001-801 Vila Real, Portugal; Tel:

+351 259 350 317; [rouboa@seas.upenn.edu](mailto:rouboa@seas.upenn.edu)

---

\*Corresponding author at: School of Mechanical Engineering, Iran University of Science and Technology, Tehran 16846 13114, Iran.

Tel: +98 9183171388 +98 8138338287 fax: +98 21 73021585.

E-mail address: : [j\\_afshari\\_m@yahoo.com](mailto:j_afshari_m@yahoo.com)

27 **Abstract**

28 Traumatic brain injury (TBI) is one of the most important causes of death and  
29 disability. The objective of this study is to develop new head injury criteria which can  
30 predict the greatest principal strain and shear stress in the brain considering the  
31 impact directions and magnitudes. So, 150 head impact simulations were performed  
32 for 3 magnitudes and 50 directions of impact using head finite element model (FEM).  
33 Simulations were performed in order to assess the strain and shear stress created in  
34 the brain tissues due to different impact directions and magnitudes. Next, new head  
35 injury criteria were developed through performing statistical analysis. The simulation  
36 results showed that TBI risks in the sagittal and frontal planes were higher than  
37 those with impacts in transverse plane. Furthermore, new brain injury indices were  
38 developed to predict maximum principal strain and shear stress in the brain, which  
39 had correlation coefficients of 0.85 and 0.89 with head FEM responses, respectively.  
40 However, finding of present research showed the effects of impact directions on TBI  
41 risks. They also demonstrate that impact magnitude, direction, and duration should  
42 be used to develop a brain injury index.

43

44

45 **Keywords:** Brain injury; Computational modeling; Finite Element Method; Injury  
46 Criteria; Safety.

47

48

49

50

51

52

53

54

55

56

57

58

59

## 60        **1- Introduction**

61        Traumatic brain injury (TBI) is one of the most important causes of death and  
62        disability. TBIs often decreases persons' ability to function and interact socially [1].  
63        Almost 1.7 million cases of TBI per year are reported in the United States[2]. As an  
64        example, about 170 000 TBI events occur in Canada every year, which the elderly  
65        and children being the frequent victims[3]. These injuries decrease ability and  
66        productivity of those who are not able to work. These TBI reports are underestimated  
67        because almost 25% of all mild and moderate cases are not included in these  
68        medical reports and many concussions do not come under clinical attention. The  
69        most important cause of TBI is falls, followed by vehicle events and striking  
70        accidents in which a person is hit by an object. TBIs may also occur during military  
71        events, vehicle crashes, and sport events [1,4–8]. This study aims to better  
72        understand the head injury mechanisms.

73        Various studies have been performed on brain injury to decrease TBI risks,  
74        which is facilitated by understanding those factors playing important roles in causing  
75        such injuries, including what characteristics an event should have in order to cause a  
76        head injury [9–12]. Head responses during impacts were measured using helmet-  
77        mounted accelerometers[13,14]. Moreover, determination of types of head impacts  
78        causing such injury can be one of the main areas of research [15–17]. Any types of  
79        TBI can be evaluated based on the events by identifying the effects of certain  
80        impacts and directions on TBIs. Furthermore, this knowledge will help designers and  
81        engineers make new protective devices and safer equipment being used to decrease  
82        TBI risks.

83        Most of injury criteria based on head kinetics are obtained from experimental  
84        results; therefore, they have become a basis for many head injury protocols,  
85        including vehicle safety standards and helmet design standards[18–22]. Head Injury  
86        Criterion (HIC) [18] and Gadd Severity Index (GSI) [19] are applied to predict TBI  
87        risks based on weighted integrals of translational acceleration-time during impacts.  
88        But, Brain Injury Criterion (BRIC) evaluates head injury using head rotational  
89        kinematics [20]. Rowson proposed injury risk curves for TBIs based on translational  
90        and rotational impacts based on injury events among collegiate athletes [23]. These  
91        head injury criteria are usually calculated to assess TBI risks by using impact time  
92        and magnitude without considering the impact orientation. Therefore, these criteria  
93        do not show any differences between the input impacts with the different directions

94 and identical profiles for TBI risks. Some researchers demonstrated that impact  
95 directions should be considered as predicting TBI risks because human head is  
96 composed of geometries with varying material properties [24–27].

97 Research done on cadavers and test animals has shown the effects of impact  
98 directions on the TBI risks [28]. The use of the animal studies for human subjects  
99 has many limitations. Coronal impact effects on the brain reactions were studied by  
100 Gennarelli et al [25], who also assessed the effects of sagittal plane impacts on the  
101 brain injury. Also, some research has been done by Kleiven [29] and Huang et al [30]  
102 to identify the effects of impact directions on TBI risks by using FEM simulations in  
103 the sagittal plane. Although some studies have shown impact orientation effects, few  
104 studies demonstrated the effects of impact directions on human brain injury  
105 considering human anatomical aspects.

106 Finite element simulations have been used to study the relationships between  
107 head kinetics and TBIs. Also, investigation of the brain reactions and prediction of  
108 TBI risks have been performed using finite element head models in soccer events,  
109 motor vehicle crashes, falls, and other impact scenarios[20,31–33]. Brain stress and  
110 strain responses in FEM are very useful tools to study TBI risks [34–39]. Although  
111 FEM is a useful tool to study TBI risks by taking impact directions into consideration,  
112 it is time-consuming. So, kinematic-based head injury criteria should be proposed to  
113 prevent head injury and predict brain stress and stress responses like finite element  
114 head models.

115 In this study, the relationships between brain reactions and head kinematics  
116 were evaluated using a 3D FE human head model in different anatomical planes.  
117 Therefore, relationships between impact directions and acceleration magnitudes with  
118 TBI risks based on maximum principal strain and shear stress were investigated  
119 using 150 FE head impact simulations. Finally, statistical analysis was performed to  
120 propose maximum principal strain criteria and shear stress criteria for predicting  
121 brain reactions.

122

## 123 **2- Method**

### 124 **2-1 Head Finite Element Model**

125 Horgan and Gilchrist's head model was applied to create the finite element  
126 head model. Their initial head FEM involved brain, specific subarachnoid for cerebro-  
127 spinal fluid (CSF), tentorium cerebral, falx cerebri, skull and face. In original Horgan

128 and Gilchrist's FE head model, skull, facial bone, CSF, dura mater, pia mater, and  
 129 combined properties of the grey and white matter of the brain were modeled using  
 130 brick, shell, brick, shell, membrane, and brick elements, respectively. [27,40].  
 131 Different anatomic layers were applied to this original model to improve the 3D  
 132 model in accurate modeling of head layers. The improved model had scalp, three  
 133 layer skull including cortical and spongy bone, dura mater, trabeculae and CSF  
 134 under subarachnoid, pia mater, tentorium cerebral, falx cerebri, brain and face[26].  
 135 The improved model consisted of 27031 elements including 7107 shell elements  
 136 and 19924 hexahedral elements. An illustration of improved FEM is given in Fig. 1.  
 137 Detailed mechanical properties of all components of this head model are illustrated  
 138 in Table 1.

139 Cortical and spongy bone, dura mater, arachnoid and pia mater were defined to  
 140 Abaqus software (Abaqus is a commercial software package for finite element  
 141 analysis, which developed by Dassault Systemes used in various disciplines of  
 142 Engineering) by Prony series to control large deformations[27]. Other parts of the  
 143 model were considered as being linear elastic. For viscoelastic section, the  
 144 relaxation shear modulus  $G_R(t)$  was introduced in ABAQUS software by  
 145 dimensionless function  $g_r(t)$  expressed by Prony series by Equation 1. Zhao work  
 146 group [41] has developed the following Equation 1:

$$g_r(t) = 1 - \sum_{i=1}^N G_i [1 - \exp(-t / \tau_i)] \quad (1)$$

147 Where  $G_0$  is the instantaneous shear modulus,  $g_r(t) = G_R(t)/G_0$  and  $\tau_i$  is  
 148 stress relaxation time. When the time  $t$  takes an infinite value, long time shear  
 149 modulus is calculated as Equation 2[26].

$$G_\infty = G_R(\infty) = g_r(\infty) \times G_0 \quad (2)$$

150 The improved model was validated by the results of two research works by  
 151 Nahum including impact along the mass center of the head and by Trosseille  
 152 including off center impact in order to validate brain reactions. Six samples of Nahum  
 153 test (1977) were applied to validate pressure prediction in finite element head model  
 154 [42]. Moreover, the Trosseille MS 428\_2 test (1992) was applied to validate the brain  
 155 response with the cadaver that was in a seated position and impacted by a 23.4 kg  
 156 hammer with 7 m/s velocities in the anterior posterior direction[27,43].

157

158  
159  
160  
161  
162  
163  
164  
165  
166  
167  
168  
169  
170  
171  
172  
173  
174  
175  
176  
177  
178  
179  
180  
181  
182  
183  
184  
185  
186  
187  
188

## 2-2 Injury Criteria for traumatic brain injury (TBI)

The injury criteria for TBI were divided into those that relate to the motion of the whole head (macro scale) and those that relate to the deformation of tissues within the head (tissue level). The macro-scale criteria are measured in experimental studies; therefore, they have become a basis for numerous head injury events. Tissue level thresholds have been measured using finite element models[22].

HIC (Head injury criteria) is one of the most important macro-scale injury criteria that was improved and advanced upon SI (Severity Index) by Versace (1971)[18]. It is the current injury index for head injury used in the FMVSS 208 standard. The HIC equation is defined as equation 3.

$$HIC = \max \left( (t_2 - t_1) \left( \frac{1}{t_2 - t_1} \int_{t_1}^{t_2} a(t) dt \right)^{2.5} \right) \tag{3}$$

Where  $a(t)$  is the resultant linear acceleration at the head center of gravity,  $t_1$  and  $t_2$  are the initial and final times, respectively, by which HIC is calculated ( $t_1$  and  $t_2$  are selected to maximize HIC). The HIC value should be limited below 1000 for preventing serious brain injury[18].

Several tissue level injury criteria have been proposed to predict injury in brain finite element models. Most of these criteria have been investigated by reconstructing real life accidents using anthropomorphic test devices and finite element head models. These reconstructed brain trauma events include falls, hockey collisions, pedestrian accidents, soccer events, and vehicle accidents, and crashes. Developed injury criteria usually use stress and strain values. Although FE head models have different anatomical structures with different injury criteria, the similar value of brain injury tolerances have been proposed to predict TBI risks[27]. Head tissue injury criteria including maximum principal strain and shear stress were applied to investigate head trauma in this study. These criteria were selected based on previous research, in which they were proposed in order to determine brain injuries [44–47]. The proposed tolerance limit for a risk of head trauma is about 7.5kPa (KiloPascal) and 0.25 for shear stress and maximum principal strain, respectively.

## 2-3 Computational Simulations

This study was performed using the FE head model having multiple anatomic parts with various material properties and validated by the results of previous experimental data. Simulations were carried out in Abaqus software using the Dynamic Explicit method. They were performed with three different magnitude impact pulses applying about 50 different directions of impact, resulting in 150 simulations (Tables 2, 3). using a cube as an example, translational impacts were applied on each of the following 50 vectors: 8 vectors from the center to the middle of each cube face, 8 vectors from the center to the cube corners, 12 vectors from the center to the midpoint of each cube edge, and 24 vectors from the center to the middle between the middle of each cube face and each cube edge (Figs. 2; Table 3)[27]. The spherical coordinate system  $(r, \theta, \varphi)$  was used to describe the impact orientations, as illustrated in Figure 2, where Z and X axes were aligned with superior and anterior directions in the head, respectively. Translational accelerations were applied to the head center of gravity as loading conditions on the skull being assumed rigid. The input load to the FE head model was an acceleration [27,42] shown in Fig. 3, which was applied with different magnitudes and directions. The model was not allowed to have a rotation in order to isolate the effects of translational direction and magnitude on response of the brain model.

## 2-4 Post-Processing of Simulations

Effects of orientation and peak linear impact on the brain responses (including principal strain and shear stress) were evaluated. Seventeen pairs of impact directions were symmetric relative to the FE head model due to the symmetry across the sagittal plane, resulting in 33 unique impact directions as shown in Table 3 [27]. To simplify the reporting of the results, only 33 unique impact orientations were evaluated while studying the principal strain and shear stress in the brain. Calculations were run in order to indicate the principal strain and shear stress responses in brain tissues due to changing the impact directions. Finally, statistical analysis was performed on the proposed new head injury metrics to predict brain reactions.

## 3- Results

### 3-1 Effects of impact parameters on brain greatest principal strain

223 The brain response diagrams show that head impact orientation has a  
224 significant effect on the brain greatest principal strain. The greatest of the maximum  
225 principal strain in the sagittal, frontal, and transverse planes occurred in the superior,  
226 superior, and posterior directions, respectively, while the minimums occurred in the  
227 inferior, inferior, and anterior directions, respectively. This finding shows that  
228 changing the impact direction in the sagittal, frontal, and transverse planes leads to  
229 changes up to 5.08, 2.89 and 1.70 times in the greatest principal strain (Figs. 4-6).  
230 Impact directions change the greatest principal strain since the head has multiple  
231 structures with varying material properties and geometries. Also, the most sensitive  
232 orientation for changing the greatest principal strain is the inferior direction in the  
233 sagittal and frontal planes because of the higher degree of relative brain/skull  
234 motions in that diction compared to others. The significantly higher value of the  
235 greatest principal strain were observed in sagittal plane simulation compared to  
236 others (Fig. 4). Value of the greatest principal strain values were lower in simulations  
237 with a pulse in the transverse plane than in others with no pulse in the transverse  
238 plane (Fig. 5). Maximum of the greatest principal strain was obtained at 0.20 in the  
239 sagittal plane, 0.20 in the frontal plane, and 0.14 in the transverse plane for the  
240 highest peak impact (R3) simulations (Figs. 4-6). For the greatest principal strain,  
241 some similar trends were calculated in three input peaks by changing impact  
242 directions.

243

### 244 **3-2 Effects of impact parameters on the brain shear stress**

245 Diagrams of the brain maximum shear stress in different planes and  
246 orientations illustrate that impact direction had a considerable effect on the brain  
247 shear stress. The gap sizes between three input magnitudes for one direction of  
248 impact in Fig. 7 show a non-linear relationship between shear stress and input  
249 peaks. Figs. 7-9 demonstrate the maximum brain shear stress in the sagittal, frontal,  
250 and transverse planes occurred in the inferior, anterior, and inferior directions while  
251 the minimums' occurred in the superior, right-left, and superior directions,  
252 respectively. Changing the impact orientations in the sagittal, frontal, and transverse  
253 planes led to changes up to 13.44, 9.06 and 10.21 times in the brain shear stress.  
254 Furthermore, sagittal plane had the highest sensitivity to changing impact directions,  
255 which was observed when the direction was changed from superior to inferior one.  
256 However, considerably greater values of maximum brain shear stress were seen in



257 simulations with the transverse plane impacts compared to those with transverse  
258 and frontal plane. These regional differences in shear stress with varied impact  
259 directions are likely due to the geometry and specific anatomy in the head model.  
260 Considerably higher values of shear stress were observed in simulations with sagittal  
261 plane impact compared to those with other planes (Fig. 7). The shear stress values  
262 in the transverse plane impact simulations were lower than those in simulations with  
263 no pulse in the transverse plane (Fig. 8). Maximum shear stress was obtained at  
264 7.29 k Pa in the sagittal plane, 7.29 k Pa in the frontal plane, and 3.49 k Pa in the  
265 transverse plane for the highest peak impact (R3) simulations. (Figs. 7-9). For shear  
266 stress, similar trends were seen in three input magnitudes by changing impact  
267 orientations.

268

### 269 **3-3 Development of new improved head injury criteria**

270 Brain injury risk, as calculated from brain MPS and shear stress, varied with  
271 impact directions and increased with an increase in the input peak for MPS and  
272 shear stress indices for any given impact directions. However, injury risk for MPS or  
273 shear stress varied with translational directions when the pulse magnitude was  
274 controlled (Table 4). The average injury risks for the highest magnitude (R1)  
275 simulations for the brain injury index were 2.77 kPa for the shear stress and 0.11 for  
276 MPS. Maximum injury risk from all simulations at the highest input peak (R1) was  
277 7.29 for brain maximum shear stress and 0.20 for brain MPS injuries. The lowest  
278 variation was observed with MPS risk at magnitude R3 with an injury risk differential  
279 of 0.10. In contrary, the highest differences were seen in shear stress risk at  
280 magnitude R1 with an injury risk differential of 6.95 kPa. Variation in injury risks due  
281 to the impact directions increased with an increase in the input magnitude. Also,  
282 variations of shear stress due to changing the impact directions were higher than  
283 brain MPS variations.

284 Non-linear relationships were seen between HIC values and input magnitudes  
285 for gap sizes of three peak pulses in each impact direction shown in Table 2. The  
286 results of the head impact FEM simulations showed that head impact directions  
287 could have a significant effect on the brain reactions. Moreover, they revealed that  
288 TBI risks can be increased by changing the impact magnitudes and HIC levels. So,  
289 effective factors were evaluated based on the findings from brain reactions  
290 (maximum brain shear stress and normal strain) by performing statistical analyses

291 on three different magnitude linear accelerations applying about 50 different  
 292 orientations, resulting in 150 simulations (Table 3). Then, the simulation results were  
 293 studied and new head injury indices were proposed in the equations 4 and 5 using  
 294 the Design Expert software. These indices included Shear Stress Criteria (equation  
 295 4) and Maximum Principal Strain Criteria (equation 5), predicting shear stress and  
 296 maximum principal strain, respectively. In these equations,  $A$  and  $B$  are defined as  
 297  $\cos \varphi$  and  $\cos \theta$  respectively. Results from regression analysis showed high  
 298 correlations between FEM simulation results and proposed brain injury indices  
 299 (Table 5). These equations predicted brain responses for head FEM with material  
 300 properties indicated in table 5.

$$SSC = ShearStressCriteria = \frac{(0.0129HIC^{0.57}) \times 100}{7.5} \times [1.11 - 1.64A - 1.36B + 0.67AB + 4.05A^2 + 0.73 \times B^2] \quad (4)$$

$$MPSC = MaximumPrincipalStrainCriteria = \frac{(0.076HIC^{0.03}) \times 100}{0.25} \times [0.11 + 0.078A - 0.029B + 0.025A^2 + 0.029A^2B - 0.016A^3 + 0.011B^3] \quad (5)$$

#### 301 4- Discussion

302 Different layers and material properties composing head geometry may affect  
 303 the brain response values during impacts with different loading directions. Present  
 304 research indicates that the highest brain stress and pressure do not occur in specific  
 305 head impact directions. Most of the injury criteria such as HIC [18] and BRIC [20]  
 306 predict TBI injury risks only through with peak accelerations, not through the  
 307 direction applied pulses. So, the risk of injury for inputs with the same acceleration  
 308 profiles will be the same regardless of impact directions. Thus, this study used FEM  
 309 simulations to investigate the effects of impact orientations and peaks for TBI injury  
 310 risks using FEM head simulations. The results clearly showed that impact directions  
 311 had significant effects on the brain reactions and head injury risks. Therefore, new  
 312 brain injury indices should take impact directions into consideration. New head injury  
 313 criteria were developed in present research using HIC to predict intracranial  
 314 responses and TBI risks considering impact directions, magnitudes and time.  
 315 Moreover, previous head injury criteria could not determine how inputs affected brain  
 316 reactions, only being capable of assessing TBI risks. But, newly developed head

317 injury criteria, including MPSC and SSC, can be applied to determine the maximum  
318 principal strain and shear stress in different head impact incidents. Findings of  
319 Previous studies are consistent with the results of the present research, showing that  
320 motions in the sagittal direction exert strains and stresses on the brain, causing high  
321 TBI risks [35]. These stresses and strains are created by a high degree of relative  
322 brain/skull motions. This is why impacts on the head sides result in fewer TBI risks  
323 and, in general, need higher pulse magnitudes to cause TBIs.

324

## 325 **5- Conclusion**

326 Relationships between brain reactions and orientations of head impacts were  
327 investigated using a 3D finite element head model with maximum principal strain and  
328 shear stress metrics. Results indicated that impact directions should be considered  
329 in order to determine head injury risks. Moreover, they showed that stress and strain  
330 imposed on the brain in sagittal and frontal planes were higher than those in the  
331 transverse planes. Also, analysis of head linear accelerations from different  
332 directions showed that Head Injury Criteria (HIC) should be developed for predicting  
333 TBI risks. So, new brain injury criteria were proposed using statistical analysis and  
334 head FEM to predict the brain reactions. Maximum Principal Strain Criteria (MPSC)  
335 and Shear Stress Criteria (SSC) had correlation coefficients of 0.85 and 0.89 with  
336 finite element results, respectively. The findings of this research can be used to  
337 better understand the relationships between head impact orientations with stress and  
338 strain imposed on the brain. Finally, protective equipment and safety systems may  
339 be improved to protect humans against head impact events using the results of this  
340 research.

341

## 342 **Conflicts of interest**

343 The authors declare that they have no conflicts of interest.

344

## 345 **Acknowledgments**

346 "This research received no specific grant from any funding agency in the public,  
347 commercial, or not-for-profit sectors".

348

349   **REFERENCES**

- 350   1.    Faul, M., Xu, L., Wald, M. M., and Coronado, V. G., “Traumatic brain injury in the  
351       United States”, *Atlanta, GA Natl. Cent. Inj. Prev. Control. Centers Dis. Control Prev.*  
352       (2010).
- 353   2.    Sosin, D. M., Sniezek, J. E., and Thurman, D. J., “Incidence of mild and moderate brain  
354       injury in the United States, 1991”, *Brain Inj.*, **10**(1), pp. 47–54 (1996).
- 355   3.    Styrke, J., Stålnacke, B.-M., Sojka, P., and Björnstig, U., “Traumatic brain injuries in a  
356       well-defined population: epidemiological aspects and severity”, *J. Neurotrauma*,  
357       **24**(9), pp. 1425–1436 (2007).
- 358   4.    Mccuen, E., Svaldi, D., Breedlove, K., Kraz, N., Cumiskey, B., Breedlove, E. L., Traver,  
359       J., Desmond, K. F., Hannemann, R. E., Zanath, E., Guerra, A., Leverenz, L., Talavage, T.  
360       M., and Nauman, E. A., “Collegiate women’s soccer players suffer greater  
361       cumulative head impacts than their high school counterparts”, *J. Biomech.*, pp. 1–4  
362       (2015).
- 363   5.    Greenwald, R. M., Gwin, J. T., Chu, J. J., and Crisco, J. J., “Head impact severity  
364       measures for evaluating mild traumatic brain injury risk exposure”, *Neurosurgery*,  
365       **62**(4), p. 789 (2008).
- 366   6.    Hajiaghameh, M., Seidi, M., Ferguson, J. R., and Caccese, V., “Measurement of  
367       Head Impact Due to Standing Fall in Adults Using Anthropomorphic Test Dummies”,  
368       *Ann. Biomed. Eng.*, **43**(9), pp. 2143–2152 (2015).
- 369   7.    Breedlove, K. M., Breedlove, E. L., Bowman, T. G., and Nauman, E. A., “Impact  
370       attenuation capabilities of football and lacrosse helmets”, *J. Biomech.*, **49**(13), pp.  
371       2838–2844 (2016).
- 372   8.    Weaver, A. a, Danelson, K. a, and Stitzel, J. D., “Modeling brain injury response for  
373       rotational velocities of varying directions and magnitudes.”, *Ann. Biomed. Eng.*, **40**(9),  
374       pp. 2005–18 (2012).
- 375   9.    Milne, G., Deck, C., Bourdet, N., Carreira, R. P., Allinne, Q., Gallego, A., and Willinger,  
376       R., “Bicycle helmet modelling and validation under linear and tangential impacts”, *Int.*  
377       *J. Crashworthiness*, **19**(4), pp. 323–333 (2014).
- 378   10.   Patton, D. A., McIntosh, A. S., and Kleiven, S., “The biomechanical determinants of  
379       concussion: finite element simulations to investigate tissue-level predictors of injury  
380       during sporting impacts to the unprotected head”, *J. Appl. Biomech.*, **31**(4), pp. 264–  
381       268 (2015).
- 382   11.   Rowson, S., Beckwith, J. G., Chu, J. J., Leonard, D. S., Greenwald, R. M., and Duma, S.  
383       M., “A six degree of freedom head acceleration measurement device for use in  
384       football”, *J. Appl. Biomech*, **27**(1), pp. 8–14 (2011).
- 385   12.   Lintern, T. O., Gamage, N. T. P., Bloomfield, F. H., Kelly, P., Finch, M. C., Taberner, A.  
386       J., Nash, M. P., and Nielsen, P. M. F., “Head kinematics during shaking associated with  
387       abusive head trauma”, *J. Biomech.*, **48**(12), pp. 3123–3127 (2015).
- 388   13.   Crisco, J. J., Costa, L., Rich, R., Schwartz, J. B., and Wilcox, B., “Surrogate headform  
389       accelerations associated with stick checks in girls’ lacrosse”, *J. Appl. Biomech.*, **31**(2),  
390       pp. 122–127 (2015).

- 391 14. Gabler, L. F., Crandall, J. R., and Panzer, M. B., "Assessment of Kinematic Brain Injury  
392 Metrics for Predicting Strain Responses in Diverse Automotive Impact Conditions",  
393 *Ann. Biomed. Eng.*, **44**(12), pp. 3705–3718 (2016).
- 394 15. Post, A., Hoshizaki, T. B., Gilchrist, M. D., Brien, S., Cusimano, M. D., and Marshall, S.,  
395 "The influence of acceleration loading curve characteristics on traumatic brain  
396 injury", *J. Biomech.*, **47**(5), pp. 1074–1081 (2014).
- 397 16. Kuo, C., Wu, L. C., Hammor, B. T., Luck, J. F., Cutcliffe, H. C., Lynall, R. C., Kait, J. R.,  
398 Campbell, K. R., Mihalik, J. P., Bass, C. R., and Camarillo, D. B., "Effect of the mandible  
399 on mouthguard measurements of head kinematics", *J. Biomech.*, pp. 1–9 (2016).
- 400 17. Butz, R. C., Knowles, B. M., Newman, J. A., and Dennison, C. R., "Effects of external  
401 helmet accessories on biomechanical measures of head injury risk : An ATD study  
402 using the HYBRIDIII headform", *J. Biomech.*, **48**(14), pp. 3816–3824 (2015).
- 403 18. Versace, J., *A Review of the Severity Index*, SAE Technical Paper (1971).
- 404 19. Gadd, C. W., "Use of a Weighted-Impulse Criterion for Estimating Injury Hazard", SAE  
405 Technical Paper (1966).
- 406 20. Takhounts, E. G., Hasija, V., Ridella, S. A., Rowson, S., and Duma, S. M., "Kinematic  
407 rotational brain injury criterion (BRIC)", *Proc. 22nd Enhanc. Saf. Veh. Conf. Pap.*  
408 (2011).
- 409 21. Kimpara, H. and Iwamoto, M., "Mild traumatic brain injury predictors based on  
410 angular accelerations during impacts.", *Ann. Biomed. Eng.*, **40**(1), pp. 114–26 (2012).
- 411 22. Wright, R. M., *A Computational Model for Traumatic Brain Injury Based on an Axonal  
412 Injury Criterion*, The Johns Hopkins University (2012).
- 413 23. Rowson, S., Duma, S. M., Beckwith, J. G., Chu, J. J., Greenwald, R. M., Crisco, J. J.,  
414 Brolinson, P. G., Duhaime, A.-C., McAllister, T. W., and Maerlender, A. C., "Rotational  
415 head kinematics in football impacts: an injury risk function for concussion", *Ann.*  
416 *Biomed. Eng.*, **40**(1), pp. 1–13 (2012).
- 417 24. Dikmen, S. S., Corrigan, J. D., Levin, H. S., Machamer, J., Stiers, W., and Weisskopf, M.  
418 G., "Cognitive outcome following traumatic brain injury", *J. Head Trauma Rehabil.*,  
419 **24**(6), pp. 430–438 (2009).
- 420 25. Amen, D. G., Wu, J. C., Taylor, D., and Willeumier, K., "Reversing brain damage in  
421 former NFL players: implications for traumatic brain injury and substance abuse  
422 rehabilitation", *J. Psychoactive Drugs*, **43**(1), pp. 1–5 (2011).
- 423 26. Afshari, J., Haghpanahi, M., Kalantarinejad, R., and Rouboa, A., "Biomechanical  
424 investigation of astronaut's seat geometry to reduce neck and head injuries while  
425 landing impact", *Int. J. Crashworthiness*, pp. 1–11 (2017).
- 426 27. Afshari, J., Haghpanahi, M., and Kalantarinejad, R., "Developing new brain injury  
427 criteria for predicting the intracranial response by calculating von Mises stress, coup  
428 pressure and contrecoup pressure", *J. Brazilian Soc. Mech. Sci. Eng.*, pp. 1–13 (2017).
- 429 28. Gennarelli, T. A., Thibault, L. E., Tomei, G., Wiser, R., Graham, D., and Adams, J.,  
430 "Directional dependence of axonal brain injury due to centroidal and non-centroidal  
431 acceleration", *SAE Tech. Pap.*, (872197) (1987).
- 432 29. Kleiven, S., "Influence of impact direction on the human head in prediction of

- 433 subdural hematoma”, *J. Neurotrauma*, **20**(4), pp. 365–379 (2003).
- 434 30. Huang, H.-M., Lee, M.-C., Chiu, W.-T., Chen, C.-T., and Lee, S.-Y., “Three-dimensional  
435 finite element analysis of subdural hematoma”, *J. Trauma Acute Care Surg.*, **47**(3), pp.  
436 538–544 (1999).
- 437 31. Ji, S. and Zhao, W., “A Pre-computed Brain Response Atlas for Instantaneous Strain  
438 Estimation in Contact Sports”, *Ann. Biomed. Eng.*, **43**(8), pp. 1877–1895 (2015).
- 439 32. Pasha Zanoosi, A. A., Mallakzadeh, M., and Kalantarinejad, R., “Optimal frame  
440 geometry of spacecraft seat based on multi-body dynamics modelling”, *Acta  
441 Astronaut.*, **115**, pp. 58–70 (2015).
- 442 33. Ghaffari, M., Zoghi, M., Rostami, M., and Abolfathi, N., “Fluid Structure Interaction of  
443 Traumatic Brain Injury: Effects of Material Properties on SAS Trabeculae”, *Int. J. Mod.  
444 Eng.*, **14**(2), pp. 54–62 (2014).
- 445 34. Hernandez, F., Wu, L. C., Yip, M. C., Laksari, K., Hoffman, A. R., Lopez, J. R., Grant, G.  
446 A., Kleiven, S., and Camarillo, D. B., “Six Degree-of-Freedom Measurements of Human  
447 Mild Traumatic Brain Injury.”, *Ann. Biomed. Eng.*, **43**(8), pp. 1918–34 (2015).
- 448 35. Post, A., Hoshizaki, T. B., Gilchrist, M. D., Brien, S., Cusimano, M., and Marshall, S.,  
449 “Traumatic brain injuries: the influence of the direction of impact.”, *Neurosurgery*,  
450 **76**(1), pp. 81–91 (2015).
- 451 36. Takhounts, E. G., Craig, M. J., Moorhouse, K., McFadden, J., and Hasija, V.,  
452 “Development of brain injury criteria (BrIC)”, *Stapp Car Crash J.*, **57**, p. 243 (2013).
- 453 37. Gabler, L., Crandall, J., and Panzer, M., “Investigating Brain Injury Tolerance in the  
454 Sagittal Plane Using a Finite Element Model of the Human Head”, *Int. J. Automot.*,  
455 **7**(1), pp. 37–43 (2016).
- 456 38. Eslaminejad, A., Hosseini Farid, M., Ziejewski, M., and Karami, G., “Brain Tissue  
457 Constitutive Material Models and the Finite Element Analysis of Blast-Induced  
458 Traumatic Brain Injury”, *Sci. Iran.*, pp. 0–0 (2018).
- 459 39. Saboori, P. and Sadegh, A., “Material modeling of the head’s subarachnoid space”,  
460 *Sci. Iran.*, **18**(6), pp. 1492–1499 (2011).
- 461 40. Horgan, T. J. and Gilchrist, M. D., “The creation of three-dimensional finite element  
462 models for simulating head impact biomechanics”, *Int. J. Crashworthiness*, **8**(4), pp.  
463 353–366 (2003).
- 464 41. Zhou, C., KHALIL, T. B., and King, A. I., “Viscoelastic response of the human brain to  
465 sagittal and lateral rotational acceleration by finite element analysis”, International  
466 IRCOBI Conference on the Biomechanics of Impacts, Dublin (1997).
- 467 42. Nahum, A. M., Smith, R., and Ward, C. C., “Intracranial Pressure Dynamics During  
468 Head Impact”, Stapp Car Crash Conference (1977).
- 469 43. Trosseille, X., Tarrière, C., Lavaste, F., Guillon, F., and Domont, A., “Development of a  
470 F.E.M. of the Human Head According to a Specific Test Protocol”, 36th Stapp Car  
471 Crash Conference (1992).
- 472 44. Post, A., Hoshizaki, T. B., Gilchrist, M. D., Brien, S., Cusimano, M., and Marshall, S.,  
473 “Traumatic brain injuries: the influence of the direction of impact.”, *Neurosurgery*,  
474 **76**(1), pp. 81–91 (2015).

- 475 45. Kleiven, S., "Predictors for traumatic brain injuries evaluated through accident  
476 reconstructions", *Stapp Car Crash J.*, **51**, p. 81 (2007).
- 477 46. Mao, H., Zhang, L., Jiang, B., Genthikatti, V. V., Jin, X., Zhu, F., Makwana, R., Gill, A.,  
478 Jandir, G., Singh, A., and Yang, K. H., "Development of a Finite Element Human Head  
479 Model Partially Validated With Thirty Five Experimental Cases", *J. Biomech. Eng.*, **135**,  
480 p. 111002 (2013).
- 481 47. Peng, Y., Deck, C., Yang, J., Otte, D., and Willinger, R., "A study of adult pedestrian  
482 head impact conditions and injury risks in passenger car collisions based on real-  
483 world accident data.", *Traffic Inj. Prev.*, **14**(6), pp. 639–46 (2013).

484

485

486 **Javad Afshari** holds a Ph.D. degree; he received his BS and MS degrees in Mechanical Engineering  
487 from *Bu-Ali Sina University*, Hamedan, Iran in 2007 and 2012, respectively, and a PhD degree in the  
488 same field of study from *Iran University of Science and Technology*, Tehran, Iran in 2017.  
489 His research interests include head injury, robot path planning, and mechanical engineering.

490

491

492 **Mohammad Haghpanahi** is a Professor of Mechanical and Biomechanical Engineering at School of  
493 Mechanical Engineering, *Iran University of Science and Technology*, Tehran. His research interests  
494 are Orthopedics Biomechanics, Sport Biomechanics, Vibration and Modal Analysis of Mechanical  
495 Systems and Stress Analysis of Systems by Finite Element Analysis.

496

497 **Reza Kalantarinejad** is an entrepreneur in the field of converging technologies. He's an associate  
498 professor in Aerospace Research Inst. who has conducted his Ph.D. dissertation designing a  
499 Nanobiosensor using modern quantum transport approaches. He is the founder of SHEZAN and  
500 HAMGARA corporations and co-founder of SAFE and ISMS startup companies. He has several patents  
501 and journal papers in the field of nanotechnology and biotech in particular.

502

503 **Abel Rouboa** is a professor at the engineering department of university of Trás-os-Montes e Alto  
504 Douro. Who is the lead of CFD research group (5 Ph.D., 3 Ph.D students and 5 Master students). P.I.  
505 of Biomechanics projects linked with Sport research groups of UTAD, UPorto and IST. He is the head  
506 of several RD projects on Applied and renewable energy financed by national and International  
507 funds.

508

509

510

511

512

## 513 **Figure Captions**

514 **Figure 1.** Developed finite element head model[27].

515 **Figure 2.** Directions of the input impacts, showing spherical coordinate system.

516 **Figure 3.** Kinematic input shape for translational accelerations.

517 **Figure 4.** The effects of impact directions on maximum brain normal strain in the sagittal  
518 plane.

519 **Figure 5.** The effects of impact directions on maximum brain normal strain in the transverse  
520 plane.

521 **Figure 6.** The effects of impact directions on maximum brain normal strain in the frontal  
522 plane.

523 **Figure 7.** The effects of impact directions on maximum brain shear stress in the sagittal plane.

524 **Figure 8.** The effects of impact directions on maximum brain shear stress in the transverse  
525 plane.

526 **Figure 9.** The effects of impact directions on maximum brain shear stress in the frontal plane.

### 527 **Table Captions**

528 **Table 1.** Mechanical properties of components of finite element head model[27].

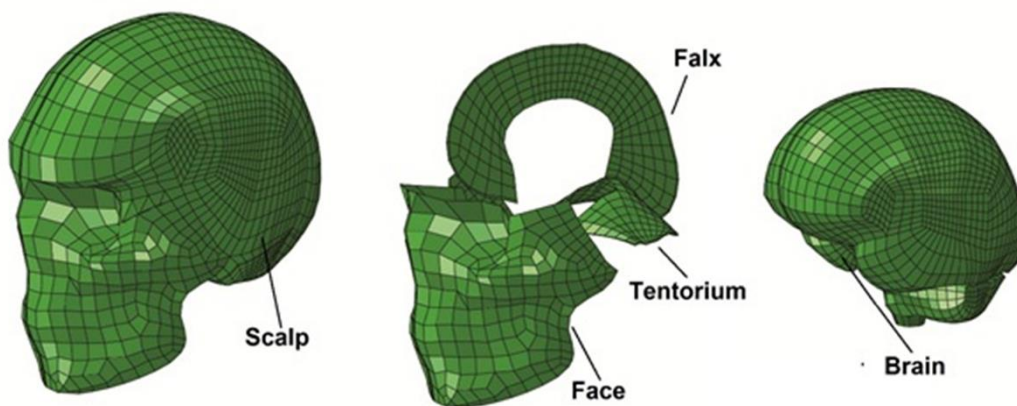
529 **Table 2.** HIC values and the peaks of linear input impacts.

530 **Table 3.** Unit vectors of applied impact directions[27].

531 **Table 4.** Summary of brain injury index grouped by input peak.

532 **Table 5.** Coefficient of determinations ( $R^2$ ) and p-values between the brain reactions and  
533 developed brain injury.

534



535



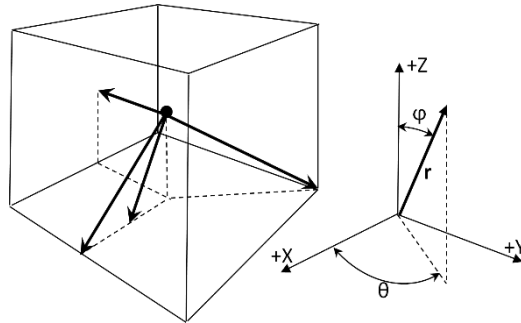
536

**Figure 1.** Developed finite element head model[27].

537

538

539

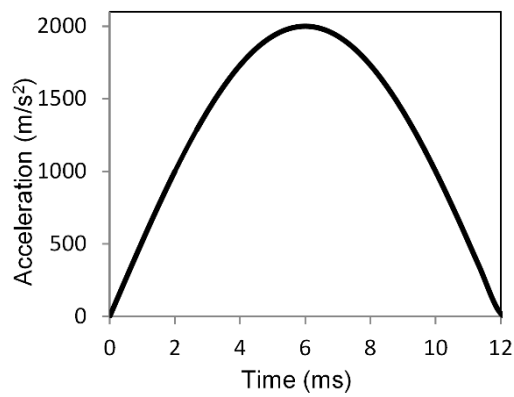


540

541

542

**Figure 2.** Directions of the input impacts, showing spherical coordinate system.

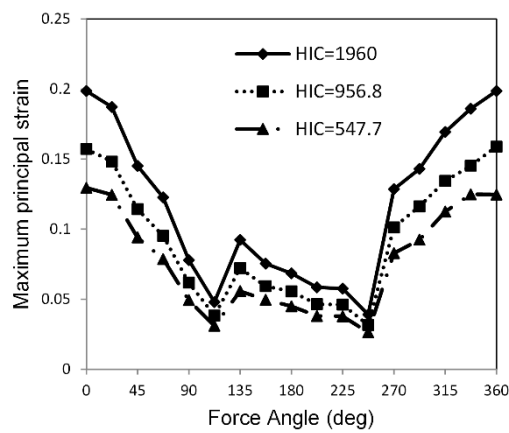


543

544

**Figure 3.** Kinematic input shape for translational accelerations.

545



546

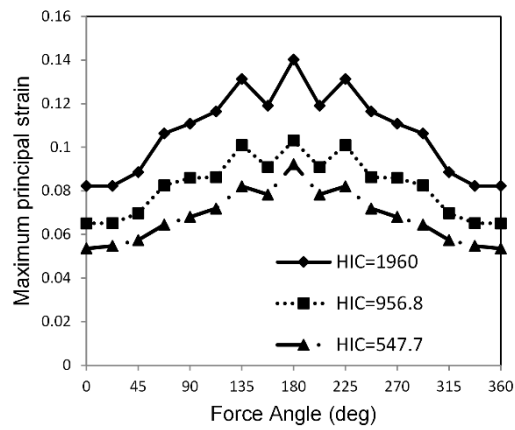
547 **Figure 4.** The effects of impact directions on maximum brain normal strain in the sagittal  
548 plane.

549

550

551

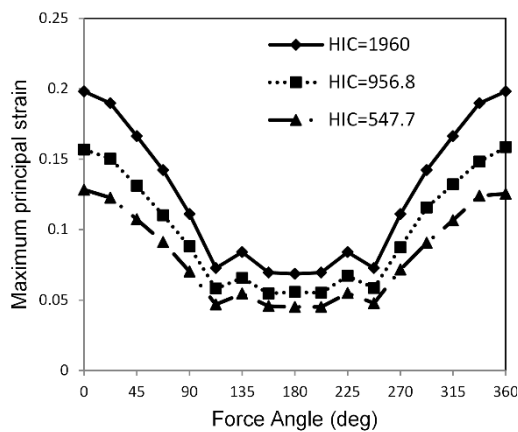
552



553

554 **Figure 5.** The effects of impact directions on maximum brain normal strain in the transverse  
555 plane.

556



557

558 **Figure 6.** The effects of impact directions on maximum brain normal strain in the frontal  
559 plane.

560

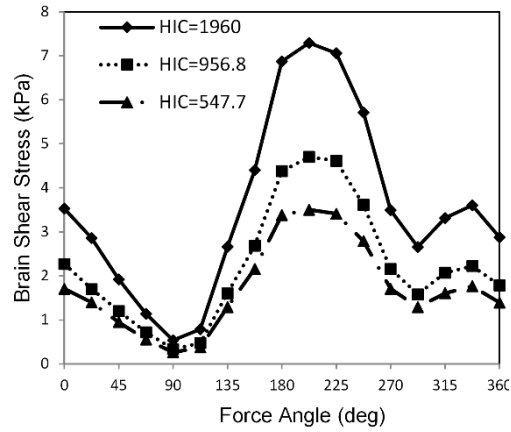
561

562

563

564

565

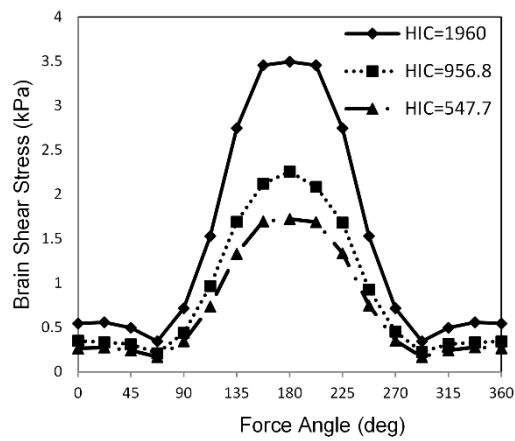


566

567 **Figure 7.** The effects of impact directions on maximum brain shear stress in the sagittal plane.

568

569



570

571 **Figure 8.** The effects of impact directions on maximum brain shear stress in the transverse  
572 plane.

573

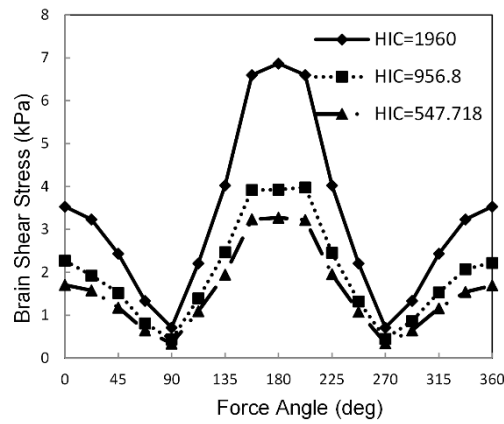
574

575

576

577

578



579

580 **Figure 9.** The effects of impact directions on maximum brain shear stress in the frontal plane.

581

582

**Table 1.** Mechanical properties of components of finite element head model[27].

Layer	Behavior	Thickness (mm)	Density (kg/m <sup>3</sup> )	Long-term elastic modulus (MPa)	Bulk modulus (MPa)	Poisson's ratio	Viscoelastic response (g <sub>R</sub> (t))
Skin	Elastic	5	1130	16.7	35	0.42	-
Cortical bone	Viscoelastic	4	2000	13000	8929	0.22	$1 - 0.0293(1 - e^{-t/9})$ $- 0.0656(1 - e^{-t/950})$ $- 0.0278(1 - e^{-t/9500})$ $- 0.107(1 - e^{-t/90.000})$
Trabecular bone	Viscoelastic	2	1300	888	740	0.3	$1$ $- 0.6224(1 - e^{-t/711.23})$ $- 0.2143(1 - e^{-t/4267.4})$
Dura mater	Viscoelastic	0.4	1140	11.72	7	0.23	$1 - 0.1088(1 - e^{-t/40})$ $- 0.0959(1 - e^{-t/10.00})$ $- 0.0922(1 - e^{-t/1000.00})$
Arachnoid mater	Viscoelastic	0.35	1130	19.32	64	0.45	$1 - 0.919(1 - e^{-t/0.002})$
CSF	Elastic	0.15	1000	0.015	2273	0.499989	-
Pia mater	Viscoelastic	0.15	1130	19.32	64	0.45	$1 - 0.919(1 - e^{-t/0.002})$
Trabeculae	Elastic	1.5	1130	0.050	22	0.48	-
Brain	Viscoelastic	-	1040	0.0228	2278	0.49998	$1 - 0.815(1 - e^{-t/0.0143})$

583

584

585

586

**Table 2.** HIC values and the peaks of linear input impacts.

Input	Peak of linear acceleration (m/s <sup>2</sup> )	HIC value
R1	2000	1960
R2	1500	956.7
R3	1200	547.7

587

588

**Table 3.** Unit vectors of applied impact directions[27].

Run	Anatomical direction	Direction	$\phi$	$\theta$	x	y	z
1	Anterior	x	90	0	1	0	0
2	Posterior	x(-)	90	180	-1	0	0
3	Left	y	90	90	0	1	0
3*	Right	y(-)	90	-90	0	-1	0
4	Superior	z	0	0	0	0	1
5	Inferior	z(-)	180	0	0	0	-1
6	Anterior- Left	x, y	90	45	0.707	0.707	0
6*	Anterior- Right	x, y(-)	90	-45	0.707	-0.707	0
7	Posterior- Left	x(-), y	90	135	-0.707	0.707	0
7*	Posterior- Right	x(-), y(-)	90	-135	-0.707	-0.707	0
8	Anterior- Superior	x, z	45	0	0.707	0	0.707
9	Posterior- Superior	x(-), z	45	180	-0.707	0	0.707
10	Anterior- Inferior	x, z(-)	135	0	0.707	0	-0.707
11	Posterior- Inferior	x(-), z(-)	135	180	-0.707	0	-0.707
12	Superior- Left	y, z	45	90	0	0.707	0.707
12*	Superior- Right	y(-), z	45	-90	0	-0.707	0.707
13	Inferior- Left	y, z(-)	135	90	0	0.707	-0.707
13*	Inferior- Right	y(-), z(-)	135	-90	0	-0.707	-0.707
14	Anterior- Left	x, y	90	22.5	0.923	0.382	0
14*	Anterior- Right	x, y(-)	90	-22.5	0.923	-0.382	0
15	Anterior- Left	x, y	90	67.5	0.382	0.923	0
15*	Anterior- Right	x, y(-)	90	-67.5	0.382	-0.923	0
16	Posterior- Left	x(-), y	90	112.5	-0.382	0.923	0
16*	Posterior- Right	x(-), y(-)	90	-112.5	-0.382	-0.923	0
17	Posterior- Left	x(-), y	90	157.5	-0.923	0.382	0
17*	Posterior- Right	x(-), y(-)	90	-157.5	-0.923	-0.382	0
18	Anterior- Superior	x, z	22.5	0	0.382	0	0.923
19	Anterior- Superior	x, z	67.5	0	0.923	0	0.382
20	Posterior- Superior	x(-), z	22.5	180	-0.382	0	0.923
21	Posterior- Superior	x(-), z	67.5	180	-0.923	0	0.382
22	Anterior- Inferior	x, z(-)	112.5	0	0.923	0	-0.382
23	Anterior- Inferior	x, z(-)	157.5	0	0.382	0	-0.923
24	Posterior- Inferior	x(-), z(-)	112.5	180	-0.923	0	-0.382
25	Posterior- Inferior	x(-), z(-)	157.5	180	-0.382	0	-0.923
26	Superior- Left	y, z	22.5	90	0	0.382	0.923
26*	Superior- Right	y(-), z	22.5	-90	0	-0.382	0.923

27	Superior- Left	y, z	67.5	90	0	0.923	0.382
27*	Superior- Right	y(-), z	67.5	-90	0	-0.923	0.382
28	Inferior- Left	y, z(-)	112.5	90	0	0.923	-0.382
28*	Inferior- Right	y(-), z(-)	112.5	-90	0	-0.923	-0.382
29	Inferior- Left	y, z(-)	157.5	90	0	0.382	-0.923
29*	Inferior- Right	y(-), z(-)	157.5	-90	0	-0.382	-0.923
30	Anterior- left- Superior	x, y, z	45	45	0.577	0.577	0.577
30*	Anterior- Right -Superior	x, y(-), z	45	-45	0.577	-0.577	0.577
31	Anterior- left- Inferior	x, y, z(-)	135	45	0.577	0.577	-0.577
31*	Anterior- Right -Inferior	x, y(-), z(-)	135	-45	0.577	-0.577	-0.577
32	Posterior - left- Superior	x(-), y, z	45	135	-0.577	0.577	0.577
32*	Posterior-Right -Superior	x(-), y(-), z	45	-135	-0.577	-0.577	0.577
33	Posterior- left- Inferior	x(-), y, z(-)	135	135	-0.577	0.577	-0.577
33*	Posterior- Right-Inferior	x(-), y(-), z(-)	135	135	-0.577	-0.577	-0.577

\* marks inputs that are symmetric relative to sagittal plane.

589

**Table 4.** Summary of brain injury index grouped by input peak.

Injury index	Input magnitude	Ave	SD	Min	Max	Differential
Shear stress (kPa)	R1	2.77	2.02	0.34	7.29	6.95
	R2	1.72	1.25	0.21	4.70	4.49
	R3	1.35	0.98	0.17	3.50	3.34
MPS	R1	0.11	0.04	0.04	0.20	0.16
	R2	0.09	0.03	0.03	0.16	0.13
	R3	0.07	0.03	0.03	0.13	0.10

590

**Table 5.** Coefficient of determinations ( $R_2$ ) and p-values between the brain reactions and developed brain injury.

Head injury criteria	Correlation coefficient	p value
MPSC	0.85	<0.001
SSC	0.89	<0.001

591